

$P_c(4457) \rightarrow P_c(4312)\pi/\gamma$ in the molecular picture

Xi-Zhe Ling,¹ Jun-Xu Lu,² Ming-Zhu Liu,^{2,1,*} and Li-Sheng Geng^{1,3,4,5,†}

¹*School of Physics, Beihang University, Beijing 102206, China*

²*School of Space and Environment, Beihang University, Beijing 102206, China*

³*Beijing Key Laboratory of Advanced Nuclear Materials and Physics,
Beihang University, Beijing 102206, China*

⁴*School of Physics and Microelectronics,
Zhengzhou University, Zhengzhou, Henan 450001, China*

⁵*Beijing Advanced Innovation Center for Big Data-Based Precision Medicine,
School of Medicine and Engineering, Beihang University, Beijing, 100191*

Abstract

The three pentaquark states, $P_c(4312)$, $P_c(4440)$, and $P_c(4457)$, discovered by the LHCb Collaboration in 2019, can be nicely arranged into a multiplet of $\bar{D}^{(*)}\Sigma_c^{(*)}$ of seven molecules dictated by heavy quark spin symmetry. In this work we employ the effective Lagrangian approach to investigate the two decay modes of $P_c(4457)$, $P_c(4457) \rightarrow P_c(4312)\pi$ and $P_c(4457) \rightarrow P_c(4312)\gamma$, via the triangle mechanism, assuming that $P_c(4457)$ and $P_c(4312)$ are $\bar{D}^*\Sigma_c$ and $\bar{D}\Sigma_c$ bound states but the spin of $P_c(4457)$ can be either 1/2 or 3/2. Our results show that the spin of $P_c(4457)$ can not be discriminated through these two decay modes. The decay widths of $P_c(4457) \rightarrow P_c(4312)\pi$ and $P_c(4457) \rightarrow P_c(4312)\gamma$ are estimated to be of order of 100 keV and 1 keV, respectively. The ratio of the partial decay widths of $P_c(4457) \rightarrow P_c(4312)\pi$ to $P_c(4457) \rightarrow P_c(4312)\gamma$ is similar to the ratio of $D^* \rightarrow D\pi$ to $D^* \rightarrow D\gamma$, which could be used to check the molecular nature of $P_c(4457)$ and $P_c(4312)$ if they can be observed in the future.

* zhengmz11@buaa.edu.cn

† lisheng.geng@buaa.edu.cn

I. INTRODUCTION:

The heavy quark spin symmetry (HQSS) dictates that the strong interaction is independent of the spin of the heavy quark in the limit of heavy quark masses [1, 2], which provides a natural explanation of the mass difference of (D, D^*) and (B, B^*) , as well as those of their baryon counterparts. In the heavy quark mass limit, D and D^* as well as Σ_c and Σ_c^* belong to the same spin doublet, which has wide implications in charm physics [3–5]. Assuming that $D_{s1}(2460)$ and $D_{s0}^*(2317)$ are D^*K and DK molecules, they can be regarded as a HQSS doublet [6, 7]. This molecule picture not only reconciles the quark model predictions [8] with the experimental measurements, but also provides a self-consistent interpretation for the mass splitting of $D_{s1}(2460)$ and $D_{s0}^*(2317)$ in terms of that of D and D^* .

It is interesting to note that in recent years, similar multiplets of hadronic molecules seem to emerge in other systems as well. In 2015, the LHCb Collaboration reported the observation of two resonant states, $P_c(4380)$ and $P_c(4450)$, in the $J/\psi p$ invariant mass distribution of the $\Lambda_b \rightarrow J/\psi p K$ decay [9]. In 2019, they updated their analysis with a data set of almost ten times bigger and found that the $P_c(4450)$ state splits into two states, $P_c(4440)$ and $P_c(4457)$, and in addition a new narrow state $P_c(4312)$ [10] emerges just below the $\bar{D}\Sigma_c$ threshold. Their masses and decay widths are

$$\begin{aligned}
 M_{P_c(4312)} &= 4311.9 \pm 0.7^{+6.8}_{-0.6} \text{ MeV} & \Gamma_{P_c(4312)} &= 9.8 \pm 2.7^{+3.7}_{-4.5} \text{ MeV}, \\
 M_{P_c(4440)} &= 4440.3 \pm 1.3^{+4.1}_{-4.7} \text{ MeV} & \Gamma_{P_c(4440)} &= 20.6 \pm 4.9^{+8.7}_{-10.1} \text{ MeV}, \\
 M_{P_c(4457)} &= 4457.3 \pm 0.6^{+4.1}_{-1.7} \text{ MeV} & \Gamma_{P_c(4457)} &= 6.4 \pm 2.0^{+5.7}_{-1.9} \text{ MeV}.
 \end{aligned} \tag{1}$$

In our previous work we showed that these states can be interpreted as $\bar{D}^{(*)}\Sigma_c$ hadronic molecules and predicted the existence of their HQSS partners in both the effective field theory (EFT) approach and the one boson exchange (OBE) model [11, 12], where a complete multiplet of seven $\bar{D}^{(*)}\Sigma_c^{(*)}$ hadronic molecules dictated by HQSS presents itself, which has later been corroborated by many studies [13–17]. Although at present the molecular interpretation is the most favored one [13–24], there exist other explanations, e.g., hadro-charmonium [25], compact pentaquark states [26–33], virtual states [34] or double triangle singularities [35]. See Refs. [36–40] for some latest reviews. As argued in Ref. [41], the most crucial, but still missing information to disentangle different interpretations is their spins.

To pin down the spins of $P_c(4440)$ and $P_c(4457)$ we can turn to other systems which are related

to the $\bar{D}^{(*)}\Sigma_c^{(*)}$ system via symmetries. In Refs. [41, 42], we extended the $\bar{D}^{(*)}\Sigma_c^{(*)}$ system to the $\Sigma_c^{(*)}\Xi_{cc}^{(*)}$ system via heavy antiquark diquark symmetry (HADS), and predicted the existence of a complete multiplet of ten triply charmed hadronic molecules. In particular, we pointed out that the mass splittings of $\Xi_{cc}\Sigma_c$ spin multiplets are correlated with the spins of $P_c(4440)$ and $P_c(4457)$, which, given the fact that the former can be much easily simulated on the lattice [43], provides a possibility to determine the spins of the later in a model independent way. After the observation of a hidden charm strange pentaquark, $P_{cs}(4459)$, with a statistical significance of 3.1 σ by the LHCb Collaboration [44], using the SU(3)-flavor symmetry we extended the $\bar{D}^{(*)}\Sigma_c^{(*)}$ system to the $\bar{D}^{(*)}\Xi_c^{(*)}$ system and predicted the existence of a multiplet of $\bar{D}^{(*)}\Xi_c^{(*)}$ hadronic molecules [45]. In addition, we found that the existence of $\bar{D}^{(*)}\Xi_c$ molecules depends on the spins of $P_c(4440)$ and $P_c(4457)$ and the light quark configurations, and we pointed out that in one scenario the existence $\bar{D}^{(*)}\Xi_c$ molecules can be used to determine the spins of $P_c(4440)$ and $P_c(4457)$.

In Refs. [18, 46], assuming that $P_c(4312)$, $P_c(4440)$, and $P_c(4457)$ are $\bar{D}^{(*)}\Sigma_c$ hadronic molecules, the authors adopted the effective Lagrangian approach to calculate the partial decay widths of three pentaquark states to $J/\psi p$ via the triangle mechanism. However, the spins of $P_c(4440)$ and $P_c(4457)$ cannot be determined. Later, the weak interaction of $\Lambda_b \rightarrow \bar{D}_s^{(*)}\Sigma_c$ was studied via the W boson emission and the production rates of three pentaquark states in the Λ_b decay were calculated, from which the spins of $P_c(4440)$ and $P_c(4457)$ cannot be determined either [22]. Following the same process, assuming that $P_{cs}(4459)$ is a $\bar{D}^*\Xi_c$ bound state with spin either 1/2 or 3/2, we calculated its production rate in the Ξ_b decay, and we found that the present experimental data cannot fully determine the $P_{cs}(4459)$ spin [47], although the decay width of a spin-3/2 P_{cs} is larger than that of a spin-1/2 one by one order of magnitude with other things being equal.

In this work, we further investigate the spin of $P_c(4457)$ via its decay into $P_c(4312)\pi$ and $P_c(4312)\gamma$. According to the LHCb measurement [10], the mass splitting between $P_c(4440)$ and $P_c(4312)$ is 128 MeV, which is less than the pion mass as shown in Fig. 1. Therefore, the decay of $P_c(4440) \rightarrow P_c(4312)\pi$ is forbidden due to phase space. The mass splitting between $P_c(4457)$ and $P_c(4312)$ is 145 MeV, accordingly the $P_c(4457) \rightarrow P_c(4312)\pi$ decay is allowed. Moreover, the radiative decays of $P_c(4457) \rightarrow P_c(4312)\gamma$ and $P_c(4440) \rightarrow P_c(4312)\gamma$ are both allowed. We note that in Refs. [48–50], assuming that $D_{s0}^*(2317)$ and $D_{s1}(2460)$ are DK and D^*K bound states, Amand Faessler, et al investigated the radiative and pionic decays of

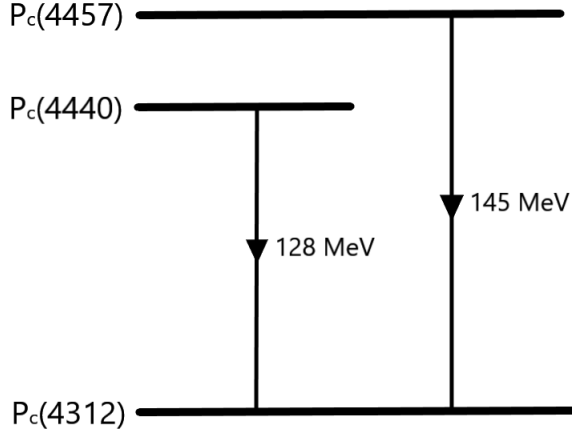


FIG. 1. Mass splittings between $P_c(4457)$, $P_c(4440)$, and $P_c(4312)$.

$D_{s1}(2317) \rightarrow D_s^* \pi / \gamma$ and $D_{s1}(2460) \rightarrow D_s^* \pi / \gamma$ together with their heavy quark spin partners, $B_{s0}^*(5725)$ and $B_{s1}(5778)$ through the effective Lagrangian approach. Subsequently, Xiao, et al used the same approach to calculate the decay widths of $D_{s1}(2460) \rightarrow D_{s1}^*(2317) \pi / \gamma$ via the triangle diagrams [51]. Based on the successful description of the strong and electromagnetic decays of $D_{s1}(2460)$ and $D_{s1}^*(2317)$, the effective Lagrangian approach is extensively applied to investigate decays of other exotic states in the molecular picture [52–56]. In the present work, assuming that $P_c(4457)$ and $P_c(4312)$ are $\bar{D}^{(*)} \Sigma_c^{(*)}$ hadronic molecules, respectively, we employ the effective Lagrangian approach to investigate the following two decay modes, $P_c(4457) \rightarrow P_c(4312) \pi$ and $P_c(4457) \rightarrow P_c(4312) \gamma$, via the triangle mechanism.

The manuscript is structured as follows. In Sec. II we present the triangle diagram of the decays of $P_c(4457) \rightarrow P_c(4312) \pi$ and $P_c(4457) \rightarrow P_c(4312) \gamma$ as well as the relevant effective Lagrangians. In Sec. III we provide the numerical results for the partial decay widths of $P_c(4457) \rightarrow P_c(4312) \pi$ and $P_c(4457) \rightarrow P_c(4312) \gamma$ and discuss their dependence on the cutoff of the regulator. Finally a brief summary is given in Sec. IV

II. THEORETICAL FORMALISM

First we explain how to construct the triangle diagram to study the decay of $P_c(4457) \rightarrow P_c(4312) \pi$. Assuming $P_c(4457)$ and $P_c(4312)$ as $\bar{D}^* \Sigma_c$ and $\bar{D} \Sigma_c$ bound states, the triangle mechanism for the $P_c(4457) \rightarrow P_c(4312) \pi$ decay is shown in Fig. 2, where the \bar{D}^* meson first decays



FIG. 2. Triangle diagram of pionic decay of $P_c(4457)$ to $P_c(4312)$ with the spin of $P_c(4457)$ being either $1/2$ or $3/2$.

into \bar{D} and π , then the \bar{D} and Σ_c interaction dynamically generates $P_c(4312)$. We note that the spin of $P_c(4457)$ is not yet known experimentally. In the molecular picture, its spin can be either $1/2$ or $3/2$ as an S -wave $\bar{D}^*\Sigma_c$ bound state. Therefore, one purpose of the present work is to check whether the pionic and radiative decay modes of $P_c(4457)$ can help us fix its spin.

Next we explain how to calculate the triangle diagram of $P_c(4457) \rightarrow P_c(4312)\pi$ in the effective Lagrangian approach. The interactions between $P_c(4312)$, $P_c(4457)^{\frac{1}{2}^-}$, and $P_c(4457)^{\frac{3}{2}^-}$, (denoted by P_{c1} , P_{c2} , and P_{c3}) and their components can be described by the following Lagrangians [18, 57],

$$\begin{aligned}\mathcal{L}_{P_{c1}\bar{D}\Sigma_c} &= -ig_{P_{c1}\bar{D}\Sigma_c}P_{c1}(x)\int dy\bar{D}(x+\omega_{\Sigma_c}y)\Sigma_c(x+\omega_{\bar{D}}y)\Phi(y^2), \\ \mathcal{L}_{P_{c2}\bar{D}^*\Sigma_c} &= g_{P_{c2}\bar{D}^*\Sigma_c}P_{c2}(x)\int dy\gamma^\mu\gamma_5\bar{D}_\mu^*(x+\omega_{\Sigma_c}y)\Sigma_c(x+\omega_{\bar{D}^*}y)\Phi(y^2), \\ \mathcal{L}_{P_{c3}\bar{D}^*\Sigma_c} &= g_{P_{c3}\bar{D}^*\Sigma_c}P_{c3}^\mu(x)\int dy\bar{D}_\mu^*(x+\omega_{\Sigma_c}y)\Sigma_c(x+\omega_{\bar{D}^*}y)\Phi(y^2),\end{aligned}\quad (2)$$

where $\omega_{\Sigma_c} = \frac{m_{\Sigma_c}}{m_{\Sigma_c}+m_{\bar{D}^{(*)}}}$ and $\omega_{\bar{D}^{(*)}} = \frac{m_{\bar{D}^{(*)}}}{m_{\Sigma_c}+m_{\bar{D}^{(*)}}}$ are the kinematic parameters with m_{Σ_c} and $m_{\bar{D}^{(*)}}$ the masses of involved particles, and $g_{P_{c1}\bar{D}\Sigma_c}$, $g_{P_{c2}\bar{D}^*\Sigma_c}$, and $g_{P_{c3}\bar{D}^*\Sigma_c}$ are the couplings between the $\bar{D}^{(*)}\Sigma_c$ molecules and their corresponding components. The correlation function $\Phi(y^2)$ is introduced to reflect the distribution of the two components in a molecule, which also renders the Feynman diagrams ultraviolet finite. Here we choose the Fourier transformation of the correlation function in form of a Gaussian function

$$\Phi(p^2) = \text{Exp}\left(-\frac{p_E^2}{\Lambda^2}\right),\quad (3)$$

where Λ is a size parameter, and P_E is the Euclidean momentum. The couplings of $g_{P_{c1}\bar{D}\Sigma_c}$, $g_{P_{c2}\bar{D}^*\Sigma_c}$, and $g_{P_{c3}\bar{D}^*\Sigma_c}$ can be estimated by reproducing the binding energies of the pentaquark states via the compositeness condition [58–60]. The condition indicates that the coupling constant

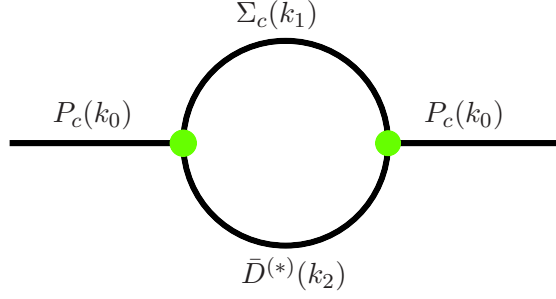


FIG. 3. Mass operators of $P_c(4312)$ and $P_c(4457)$ as $\bar{D}\Sigma_c$ and $\bar{D}^*\Sigma_c$ bound states.

can be determined from the fact that the renormalization constant of the wave function of a composite particle should be zero. For a spin-1/2 $\bar{D}^{(*)}\Sigma_c$ bound state, the compositeness condition is,

$$Z_{P_c} = 1 - \frac{d\Sigma_{P_c}(k_0)}{dk_0} \Big|_{k_0=m_{P_c}} = 0, \quad (4)$$

where $\Sigma_{P_c}(k_0)$ is the self-energy of the composite particle with spin-1/2, as illustrated in Fig 3. For a spin-3/2 $\bar{D}^*\Sigma_c$ bound state, the self energy can be divided into a transverse part and a longitudinal part, i.e.,

$$\Sigma^{\mu\nu} = g_{\perp}^{\mu\nu}\Sigma^T(k_0) + \frac{p^\mu p^\nu}{p^2}\Sigma^L(k_0). \quad (5)$$

The compositeness condition for a spin-3/2 composite particle can be estimated from its transverse part

$$Z_{P_c} = 1 - \frac{d\Sigma_{P_c}^T(k_0)}{dk_0} \Big|_{k_0=m_{P_c}} = 0. \quad (6)$$

With Eqs. (4) and (6), the $P_c(4312)$ and $P_c(4457)$ couplings to their components can be determined. With the size parameter $\Lambda=1$ GeV, the corresponding couplings are determined as $g_{P_{c1}\bar{D}\Sigma_c} = 2.294$, $g_{P_{c2}\bar{D}^*\Sigma_c} = 1.069$, $g_{P_{c3}\bar{D}^*\Sigma_c} = 1.851$, consistent with Refs. [13, 19, 22].

The Lagrangian describing the D^* decay into D and π is given by

$$\mathcal{L}_{DD^*\pi} = -ig_{DD^*\pi}(D\partial^\mu\pi D_\mu^\dagger - D_\mu^*\partial^\mu\pi D^\dagger) \quad (7)$$

where the coupling $g_{DD^*\pi}$ is determined as $g_{DD^*\pi} = 16.1$ by reproducing the decay width of $D^{*+} \rightarrow D^+\pi^0$ [61].

Utilizing all the relevant Lagrangians, the amplitude of $P_c(4457) \rightarrow P_c(4312)\pi$ of Fig. 2 can be written as

$$i\mathcal{M}_{1/2} = g_{P_{c1}\bar{D}\Sigma_c}g_{P_{c2}\bar{D}^*\Sigma_c}g_{DD^*\pi} \int \frac{d^4q}{(2\pi)^4} \bar{u}_{p_{c1}} \frac{1}{k_1 - m_{\Sigma_c}} \frac{1}{q^2 - m_D^2} p_{2\alpha} \frac{-g^{\alpha\beta} + \frac{k_2^\alpha k_2^\beta}{m_{D^*}^2}}{k_2^2 - m_{D^*}^2} \gamma_\beta \gamma_5 u_{p_{c2}} F(q^2),$$

$$i\mathcal{M}_{3/2} = g_{P_{c1}\bar{D}\Sigma_c}g_{P_{c3}\bar{D}^*\Sigma_c}g_{DD^*\pi} \int \frac{d^4q}{(2\pi)^4} \bar{u}_{p_{c1}} \frac{1}{k_1 - m_{\Sigma_c}} \frac{1}{q^2 - m_D^2} p_{2\alpha} \frac{-g^{\alpha\beta} + \frac{k_2^\alpha k_2^\beta}{m_{D^*}^2}}{k_2^2 - m_{D^*}^2} u_{p_{c3\beta}} F(q^2),$$

where $\mathcal{M}_{1/2}$ and $\mathcal{M}_{3/2}$ represent the amplitudes of $P_c(4457) \rightarrow P_c(4312)\pi$ for the cases of the $P_c(4457)$ spin being either 3/2 or 1/2, p_2 , k_1 , k_2 , and q denote the momenta of π , Σ_c , \bar{D}^* , and \bar{D} , and $u_{P_{c2}}$, $u_{P_{c3}}$, and $\bar{u}_{P_{c1}}$ are the initial and final spinors, respectively. In addition, to eliminate the ultraviolet divergence of the above amplitudes, we supplement the relevant vertices of exchanging a \bar{D} meson with the following monopolar form factor $F(q^2)$

$$F(q^2) = \frac{\Lambda^2 - m^2}{\Lambda^2 - q^2} \frac{\Lambda_1^2 - m^2}{\Lambda_1^2 - q^2}, \quad (8)$$

which also reflects the internal structure of hadrons, similar to the OBE model [62]. Since there are two different types of vertices involving \bar{D} in Fig 2, we use different cutoff values, i.e., Λ and Λ_1 , for each type of vertices. Following Ref. [63], we assume that Λ and Λ_1 are related and we study the following two scenarios to estimate the induced uncertainty, i.e., $\Lambda_1 = 0.9\Lambda$ and $\Lambda_1 = 1.1\Lambda$.

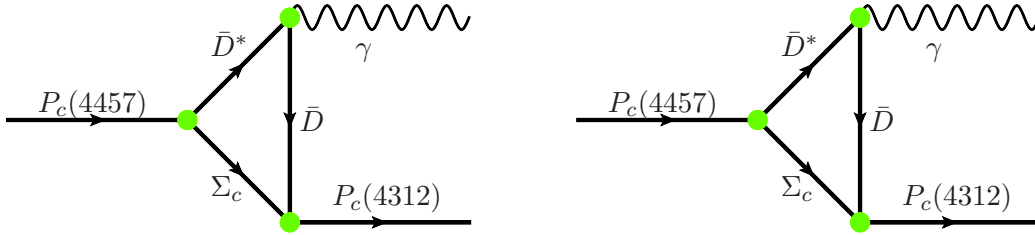


FIG. 4. Triangle diagram for the radiative decay of $P_c(4457)$ to $P_c(4312)$ with the spin of $P_c(4457)$ being either 1/2 or 3/2.

The radiative decay of $P_c(4457)[P_c(4440)] \rightarrow P_c(4312) + \gamma$ can also be investigated in the effective Lagrangian approach via the triangle mechanism shown in Fig. 4. In comparison with with the $P_c(4457) \rightarrow P_c(4312)\pi$ decay, the vertex $\bar{D}^* \rightarrow \bar{D}\pi$ in Fig. 2 is replaced with $\bar{D}^* \rightarrow \bar{D}\gamma$. The interaction between charmed mesons and the photon is described by the following Lagrangian

$$\mathcal{L}_{DD^*\gamma} = \frac{g_{DD^*\gamma}}{4} e \varepsilon^{\mu\nu\alpha\beta} F_{\mu\nu} D_{\alpha\beta}^* D = e g_{DD^*\gamma} \varepsilon^{\mu\nu\alpha\beta} \partial_\mu A_\nu \partial_\alpha D_\beta^*, \quad (9)$$

where $F_{\mu\nu} = \partial_\mu A_\nu - \partial_\nu A_\mu$ and $D_{\alpha\beta}^* = \partial_\alpha D_\beta^* - \partial_\beta D_\alpha^*$, and the fine structure constant $\frac{e^2}{4\pi} = \frac{1}{137}$. The coupling $g_{DD^*\gamma}$ is determined as 0.469 GeV^{-1} by reproducing the decay width of $D^{*+} \rightarrow D^+\gamma$ [61].

The amplitudes of the triangle diagrams in Fig. 4 can be written as

$$\begin{aligned}
i\mathcal{M}_{1/2} &= eg_{P_{c1}\bar{D}\Sigma_c}g_{P_{c2}\bar{D}^*\Sigma_c}g_{DD^*\gamma} \int \frac{d^4q}{(2\pi)^4} \bar{u}_{p_{c1}} \frac{1}{\not{k}_1 - m_{\Sigma_c}} \frac{1}{q^2 - m_{\bar{D}}^2} \varepsilon_{\mu\nu\sigma\alpha} p_2^\mu \varepsilon^\nu(p_2) k_2^\sigma \\
&\quad \frac{-g^{\alpha\beta} + \frac{k_2^\alpha k_2^\beta}{m_{\bar{D}^*}^2}}{k_2^2 - m_{\bar{D}^*}^2} \gamma_\beta \gamma_5 u_{p_{c2}} F(q^2), \\
i\mathcal{M}_{3/2} &= eg_{P_{c1}\bar{D}\Sigma_c}g_{P_{c3}\bar{D}^*\Sigma_c}g_{DD^*\gamma} \int \frac{d^4q}{(2\pi)^4} \bar{u}_{p_{c1}} \frac{1}{\not{k}_1 - m_{\Sigma_c}} \frac{1}{q^2 - m_{\bar{D}}^2} \varepsilon_{\mu\nu\sigma\alpha} p_2^\mu \varepsilon^\nu(p_2) k_2^\sigma \\
&\quad \frac{-g^{\alpha\beta} + \frac{k_2^\alpha k_2^\beta}{m_{\bar{D}^*}^2}}{k_2^2 - m_{\bar{D}^*}^2} u_{p_{c3}\beta} F(q^2),
\end{aligned}$$

where $\mathcal{M}_{1/2}$ and $\mathcal{M}_{3/2}$ are for the initial state having spin 1/2 and 3/2, respectively, p_2 , k_1 , k_2 , and q denote the momentum of photon, Σ_c , \bar{D}^* , and \bar{D} , respectively, and $u_{P_{c2}}$, $u_{P_{c3}}$, and $\bar{u}_{P_{c1}}$ represent the initial and final spinors. In the mechanism shown in Fig. 4, the radiative decay of $P_c(4457) \rightarrow P_c(4312) + \gamma$ occurs via its component \bar{D}^* . Because the vertex of $\bar{D}^* \rightarrow \bar{D}\gamma$ is gauge invariant, the whole amplitude is gauge invariant as well.

With the amplitudes of pionic and radiative decays of $P_c(4457)$ to $P_c(4312)$ determined, one can obtain the corresponding partial decay widths as

$$\Gamma = \frac{1}{2J+1} \frac{1}{8\pi} \frac{|\vec{p}|}{m_{P_c}^2} |\overline{\mathcal{M}}|^2, \quad (10)$$

where J is the total angular momentum of the initial state $P_c(4457)$, the overline indicates the sum over the polarization vectors of final states, and $|\vec{p}|$ is the momentum of either final state in the rest frame of $P_c(4457)$.

III. NUMERICAL RESULTS AND DISCUSSIONS

Before presenting the numerical results for the pionic and radiative partial decay widths, we discuss the cutoff dependence of our results. As explained above, we have introduced a monopolar form factor for the meson exchange vertices. The cutoff reflects the fact that hadrons are not pointlike particles and its value is not known a priori. In the OBE model the cutoff can be fixed by reproducing the binding energies of some molecular candidates. In our previous works [12, 15, 62], based on the molecular picture where the deuteron, $X(3872)$, and $P_c(4312)$ are nucleon-nucleon, $\bar{D}D^*$, and $\bar{D}\Sigma_c$ bound states, we fixed the corresponding cutoff of the OBE model as 0.86, 1.01, and 1.12 GeV, respectively, which can also be described by an empirical formula $\Lambda = m_E + \alpha\Lambda_{QCD}$ [64], where m_E is the most massive particle of all allowed exchange particles,

$\Lambda_{QCD} \sim 200 - 300$ MeV is the scale parameter of Quantum Chromodynamics (QCD), and α is a dimensionless parameter. In general, α is taken to be unity, and the corresponding formula is $\Lambda = m_E + \Lambda_{QCD}$. If we apply this formula to the present work, the cutoff is estimated to $\Lambda = 2.1$ GeV. In the following, to study the dependence of the results on the cutoff, we vary the cutoff from 2.1 to 2.6 GeV.

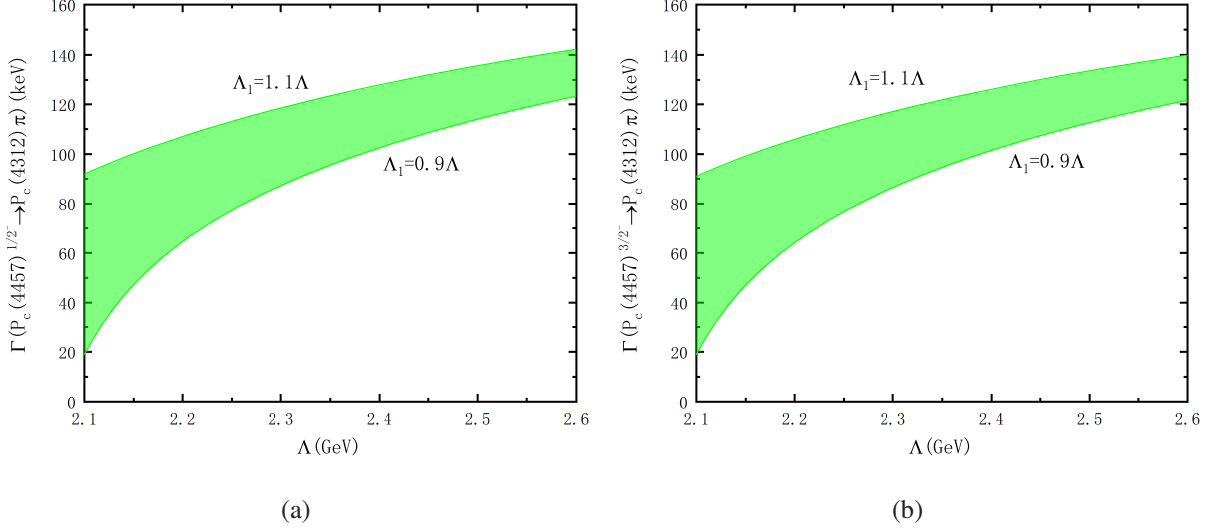


FIG. 5. Decay widths of $P_c(4457)^{1/2} \rightarrow P_c(4312)\pi$ (a) and $P_c(4457)^{3/2} \rightarrow P_c(4312)\pi$ (b) as a function of the cutoff.

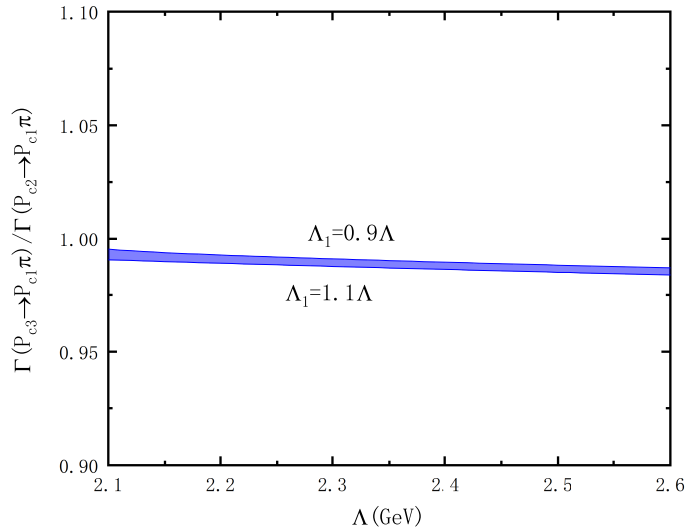


FIG. 6. Ratio of the partial decay widths of $P_c(4457)^{3/2} \rightarrow P_c(4312)\pi$ to $P_c(4457)^{1/2} \rightarrow P_c(4312)\pi$ as a function of the cutoff.

In Fig. 5 we show the decay width of $P_c(4457) \rightarrow P_c(4312)\pi$ as a function of the cutoff, where

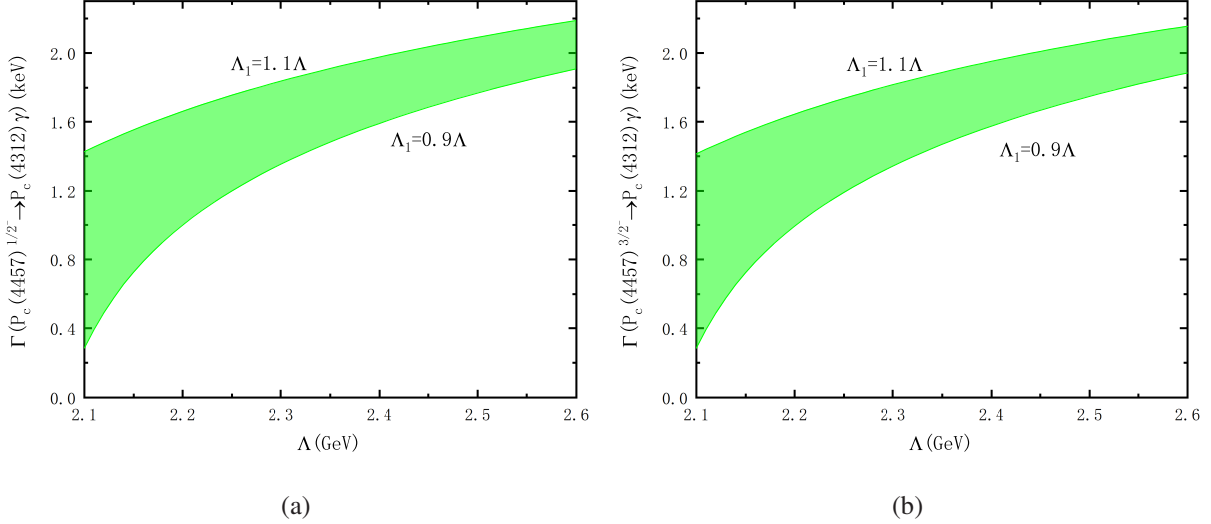


FIG. 7. Decay width of $P_c(4457)^{1/2} \rightarrow P_c(4312)\gamma$ (a) and $P_c(4457)^{3/2} \rightarrow P_c(4312)\gamma$ (b) as a function of the cutoff.

Fig. (1a) is for spin-1/2, and Fig. (1b) for spin-3/2. As the cutoff varies from 2.1 to 2.6 GeV, the decay width of $P_c(4457)^{\frac{1}{2}^-} \rightarrow P_c(4312)\pi$ changes from 91.7 keV to 142.2 keV with $\Lambda_1 = 1.1\Lambda$ and from 18.8 keV to 123.2 keV with $\Lambda_1 = 0.9\Lambda$, while the decay width of $P_c(4457)^{\frac{3}{2}^-} \rightarrow P_c(4312)\pi$ changes from 90.9 keV to 139.8 keV with $\Lambda_1 = 1.1\Lambda$ and from 18.7 keV to 121.5 keV with $\Lambda_1 = 0.9\Lambda$. The decay widths of $P_c(4457) \rightarrow P_c(4312)\pi$ for spin 1/2 and 3/2 are close to each other, with the latter a bit larger, which can be explicitly seen from the ratio of the decay width of a spin-3/2 $P_c(4457)$ to that of a spin-1/2 $P_c(4457)$ shown in Fig. 6. Our results show that the spin of $P_c(4457)$ can not be discriminated from the $P_c(4457) \rightarrow P_c(4312)\pi$ decay. The decay width of $P_c(4457) \rightarrow P_c(4312)\pi$ is predicted to be of order of 100 keV in the molecular picture. In comparison with the total decay width of $P_c(4457)$, the branching ratio of $P_c(4457) \rightarrow P_c(4312)\pi$ is 1.5%. With more data accumulated, the LHCb Collaboration should be able to observe the decay of $P_c(4457) \rightarrow P_c(4312)\pi$.

For the radiative decay, both $P_c(4457)$ and $P_c(4440)$ can decay into $P_c(4312)$. The spin of $P_c(4440)$ can be either 1/2 or 3/2 as a $\bar{D}^*\Sigma_c$ bound state, thus yielding similar results as the $P_c(4457)$ for the radiative decay, except for the small difference originating from the slightly different phase space. Therefore, we refrain from explicitly presenting the numerical results of $P_c(4440) \rightarrow P_c(4312)\gamma$. The partial decay width of $P_c(4457) \rightarrow P_c(4312)\gamma$ as a function of the cutoff is shown in Fig. 7, where the left and right figures are for the spin-1/2 and spin-3/2 assignments for the initial state $P_c(4457)$, respectively. One can see that the decay widths are

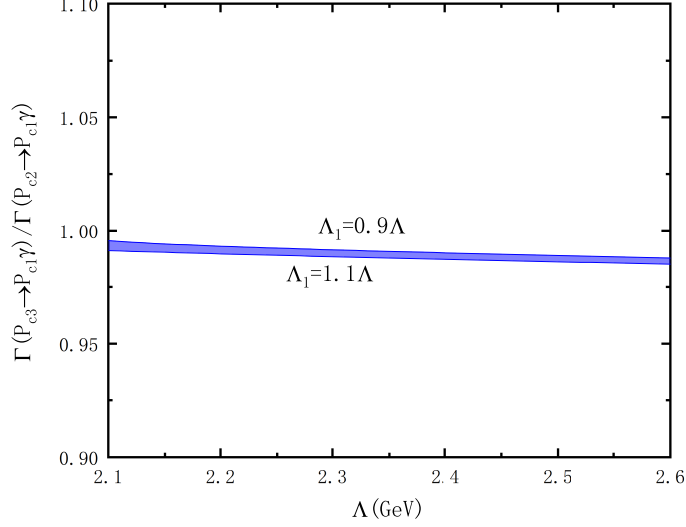


FIG. 8. Ratio of the decay width of $P_c(4457)^{3/2} \rightarrow P_c(4312)\gamma$ to $P_c(4457)^{1/2} \rightarrow P_c(4312)\gamma$ as a function of the cutoff.

close to each other. In Fig. 8 the ratio of the partial decay width of $P_c(4457)^{3/2} \rightarrow P_c(4312)\gamma$ to $P_c(4457)^{1/2} \rightarrow P_c(4312)\gamma$ is presented, which shows that the partial decay width for spin-3/2 is a bit larger than that for spin 1/2. Similar to the pionic decay mode, the radiative decay mode cannot be employed to distinguish the two spin assignments for $P_c(4457)$. As the cutoff varies from 2.1 to 2.6 GeV, the decay width of $P_c(4457)^{\frac{1}{2}-} \rightarrow P_c(4312)\gamma$ changes from 1.4 keV to 2.2 keV with $\Lambda_1 = 1.1\Lambda$ and from 0.3 keV to 1.9 keV with $\Lambda_1 = 0.9\Lambda$, while the decay width of $P_c(4457)^{\frac{3}{2}-} \rightarrow P_c(4312)\gamma$ changes from 1.4 keV to 2.2 keV with $\Lambda_1 = 1.1\Lambda$ and from 0.3 keV to 1.9 keV with $\Lambda_1 = 0.9\Lambda$. Compared with the total decay width of $P_c(4457)$, the corresponding branching ratio is about 0.02%.

Finally, the ratio of the partial decay width of $P_c(4457) \rightarrow P_c(4312)\gamma$ to $P_c(4457) \rightarrow P_c(4312)\pi$ is given in Fig. 9, where the left and right figures are for spin-1/2 and spin-3/2 assignments, respectively. The ratio is about 1.5% in the two cases, in agreement with the ratio of the decay width of $D^* \rightarrow D\gamma$ to $D^* \rightarrow D\pi$ [61],

$$\frac{Br(P_c(4457) \rightarrow P_c(4312)\gamma)}{Br(P_c(4457) \rightarrow P_c(4312)\pi)} \approx \frac{Br(D^* \rightarrow D\gamma)}{Br(D^* \rightarrow D\pi)} \sim 1.6\%, \quad (11)$$

which illustrates that the radiative and pionic decays of charmed mesons may play an important role in describing the radiative and pionic decays of $P_c(4457)$. In other words, $P_c(4457)$ and $P_c(4312)$ contain large molecular components, which reminds us of the fact that the mass splitting of $D_{s0}^*(2317)$ and $D_{s1}(2460)$ can be easily understood in the DK and D^*K molecular picture.

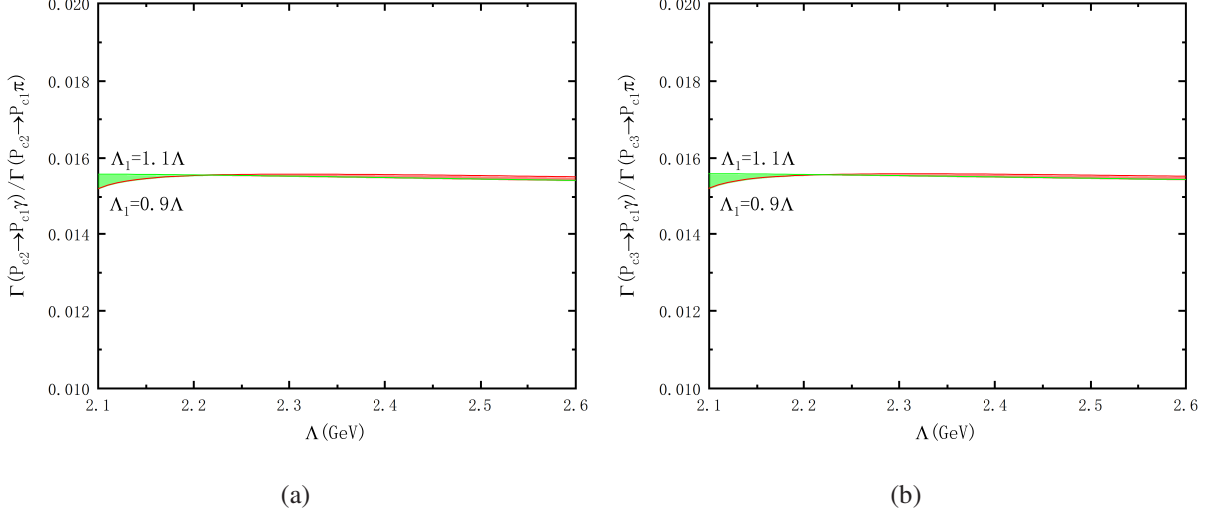


FIG. 9. Ratio of the radiative decay width and the pionic decay width of $P_c(4457)$ as a function of the cutoff.

Therefore, if the ratio of $P_c(4457) \rightarrow P_c(4312)\gamma$ to $P_c(4457) \rightarrow P_c(4312)\pi$ is observed in future experiments, it will help us to either confirm or repute the molecular nature of $P_c(4457)$ and $P_c(4312)$.

IV. SUMMARY

In this work, assuming $P_c(4457)$ and $P_c(4312)$ as $\bar{D}^{(*)}\Sigma_c^{(*)}$ hadronic molecules, we employ the effective Lagrangian approach to investigate the decays of $P_c(4457) \rightarrow P_c(4312)\pi$ and $P_c(4457) \rightarrow P_c(4312)\gamma$ via the triangle mechanism. With the assignment for the spin of $P_c(4457)$ as either 1/2 and 3/2 we found the decay width of $P_c(4457) \rightarrow P_c(4312)\pi$ is at the order of 100 keV, and the decay width of $P_c(4457) \rightarrow P_c(4312)\gamma$ is at the order of 1.5 keV. In comparison with the total decay width of $P_c(4457)$, we obtained the branching ratios of $P_c(4457) \rightarrow P_c(4312)\pi$ and $P_c(4457) \rightarrow P_c(4312)\gamma$, i.e., 1.5% and 0.02%, respectively. With a larger statistics, it is likely that the LHCb Collaboration could observe the $P_c(4457) \rightarrow P_c(4312)\pi$ decay. The ratio of $P_c(4457) \rightarrow P_c(4312)\gamma$ to $P_c(4457) \rightarrow P_c(4312)\pi$ is 1.5%, consistent with the ratio of $D^* \rightarrow D\gamma$ to $D^* \rightarrow D\pi$, which can be easily understood in the molecular picture where $P_c(4457)$ and $P_c(4312)$ are $\bar{D}^*\Sigma_c$ and $\bar{D}\Sigma_c$ molecules, respectively. In addition we found that the spin of $P_c(4457)$ can not be discriminated through these two decay modes, $P_c(4457) \rightarrow P_c(4312)\pi$ and $P_c(4457) \rightarrow P_c(4312)\gamma$.

V. ACKNOWLEDGMENTS

This work is partly supported by the National Natural Science Foundation of China under Grants Nos.11735003, 11975041, and 11961141004, and the fundamental Research Funds for the Central Universities.

-
- [1] N. Isgur and M. B. Wise, Phys. Lett. **B232**, 113 (1989).
 - [2] N. Isgur and M. B. Wise, Phys. Lett. **B237**, 527 (1990).
 - [3] T.-M. Yan, H.-Y. Cheng, C.-Y. Cheung, G.-L. Lin, Y. C. Lin, and H.-L. Yu, Phys. Rev. **D46**, 1148 (1992), [Erratum: Phys. Rev. **D55**, 5851(1997)].
 - [4] H.-Y. Cheng, C.-Y. Cheung, G.-L. Lin, Y. C. Lin, T.-M. Yan, and H.-L. Yu, Phys. Rev. D **47**, 1030 (1993), arXiv:hep-ph/9209262.
 - [5] R. Casalbuoni, A. Deandrea, N. Di Bartolomeo, R. Gatto, F. Feruglio, and G. Nardulli, Phys. Rept. **281**, 145 (1997), arXiv:hep-ph/9605342.
 - [6] F.-K. Guo, P.-N. Shen, and H.-C. Chiang, Phys. Lett. **B647**, 133 (2007), arXiv:hep-ph/0610008 [hep-ph].
 - [7] M. Altenbuchinger, L. S. Geng, and W. Weise, Phys. Rev. **D89**, 014026 (2014), arXiv:1309.4743 [hep-ph].
 - [8] S. Godfrey and N. Isgur, Phys. Rev. **D32**, 189 (1985).
 - [9] R. Aaij et al. (LHCb), Phys. Rev. Lett. **115**, 072001 (2015), arXiv:1507.03414 [hep-ex].
 - [10] R. Aaij et al. (LHCb), Phys. Rev. Lett. **122**, 222001 (2019), arXiv:1904.03947 [hep-ex].
 - [11] M.-Z. Liu, Y.-W. Pan, F.-Z. Peng, M. Sánchez Sánchez, L.-S. Geng, A. Hosaka, and M. Pavon Valderrama, Phys. Rev. Lett. **122**, 242001 (2019), arXiv:1903.11560 [hep-ph].
 - [12] M.-Z. Liu, T.-W. Wu, M. Pavon Valderrama, J.-J. Xie, and L.-S. Geng, Phys. Rev. **D99**, 094018 (2019), arXiv:1902.03044 [hep-ph].
 - [13] C. W. Xiao, J. Nieves, and E. Oset, Phys. Rev. **D100**, 014021 (2019), arXiv:1904.01296 [hep-ph].
 - [14] Y. Yamaguchi, H. García-Tecocoatzi, A. Giachino, A. Hosaka, E. Santopinto, S. Takeuchi, and M. Takizawa, Phys. Rev. **D101**, 091502 (2020), arXiv:1907.04684 [hep-ph].
 - [15] M.-Z. Liu, T.-W. Wu, M. Sánchez Sánchez, M. P. Valderrama, L.-S. Geng, and J.-J. Xie, Phys. Rev. **D103**, 054004 (2021), arXiv:1907.06093 [hep-ph].

- [16] M. Pavon Valderrama, Phys. Rev. **D100**, 094028 (2019), arXiv:1907.05294 [hep-ph].
- [17] M.-L. Du, V. Baru, F.-K. Guo, C. Hanhart, U.-G. Meißner, J. A. Oller, and Q. Wang, Phys. Rev. Lett. **124**, 072001 (2020), arXiv:1910.11846 [hep-ph].
- [18] C.-J. Xiao, Y. Huang, Y.-B. Dong, L.-S. Geng, and D.-Y. Chen, Phys. Rev. D **100**, 014022 (2019), arXiv:1904.00872 [hep-ph].
- [19] S. Sakai, H.-J. Jing, and F.-K. Guo, Phys. Rev. **D100**, 074007 (2019), arXiv:1907.03414 [hep-ph].
- [20] L. Meng, B. Wang, G.-J. Wang, and S.-L. Zhu, Phys. Rev. D **100**, 014031 (2019), arXiv:1905.04113 [hep-ph].
- [21] T. J. Burns and E. S. Swanson, Phys. Rev. D **100**, 114033 (2019), arXiv:1908.03528 [hep-ph].
- [22] Q. Wu and D.-Y. Chen, Phys. Rev. D **100**, 114002 (2019), arXiv:1906.02480 [hep-ph].
- [23] K. Azizi, Y. Sarac, and H. Sundu, Chin. Phys. **C45**, 053103 (2021), arXiv:2011.05828 [hep-ph].
- [24] K. Phumphan, W. Ruangyoo, C.-C. Chen, A. Limphirat, and Y. Yan, (2021), arXiv:2105.03150 [hep-ph].
- [25] M. I. Eides, V. Y. Petrov, and M. V. Polyakov, Mod. Phys. Lett. **A35**, 2050151 (2020), arXiv:1904.11616 [hep-ph].
- [26] A. Ali and A. Y. Parkhomenko, Phys. Lett. B **793**, 365 (2019), arXiv:1904.00446 [hep-ph].
- [27] H. Mutuk, Chin. Phys. C **43**, 093103 (2019), arXiv:1904.09756 [hep-ph].
- [28] Z.-G. Wang, Int. J. Mod. Phys. A **35**, 2050003 (2020), arXiv:1905.02892 [hep-ph].
- [29] J.-B. Cheng and Y.-R. Liu, Phys. Rev. **D100**, 054002 (2019), arXiv:1905.08605 [hep-ph].
- [30] X.-Z. Weng, X.-L. Chen, W.-Z. Deng, and S.-L. Zhu, Phys. Rev. **D100**, 016014 (2019), arXiv:1904.09891 [hep-ph].
- [31] R. Zhu, X. Liu, H. Huang, and C.-F. Qiao, Phys. Lett. **B797**, 134869 (2019), arXiv:1904.10285 [hep-ph].
- [32] A. Pimikov, H.-J. Lee, and P. Zhang, Phys. Rev. **D101**, 014002 (2020), arXiv:1908.04459 [hep-ph].
- [33] W. Ruangyoo, K. Phumphan, C.-C. Chen, A. Limphirat, and Y. Yan, (2021), arXiv:2105.14249 [hep-ph].
- [34] C. Fernández-Ramírez, A. Pilloni, M. Albaladejo, A. Jackura, V. Mathieu, M. Mikhasenko, J. A. Silva-Castro, and A. P. Szczepaniak (JPAC), Phys. Rev. Lett. **123**, 092001 (2019), arXiv:1904.10021 [hep-ph].
- [35] S. X. Nakamura, (2021), arXiv:2103.06817 [hep-ph].

- [36] Y.-R. Liu, H.-X. Chen, W. Chen, X. Liu, and S.-L. Zhu, *Prog. Part. Nucl. Phys.* **107**, 237 (2019), arXiv:1903.11976 [hep-ph].
- [37] N. Brambilla, S. Eidelman, C. Hanhart, A. Nefediev, C.-P. Shen, C. E. Thomas, A. Vairo, and C.-Z. Yuan, *Phys. Rept.* **873**, 1 (2020), arXiv:1907.07583 [hep-ex].
- [38] F.-K. Guo, X.-H. Liu, and S. Sakai, *Prog. Part. Nucl. Phys.* **112**, 103757 (2020), arXiv:1912.07030 [hep-ph].
- [39] G. Yang, J. Ping, and J. Segovia, *Symmetry* **12**, 1869 (2020), arXiv:2009.00238 [hep-ph].
- [40] X.-K. Dong, F.-K. Guo, and B.-S. Zou, *Progr. Phys.* **41**, 65 (2021), arXiv:2101.01021 [hep-ph].
- [41] Y.-W. Pan, M.-Z. Liu, F.-Z. Peng, M. Sánchez Sánchez, L.-S. Geng, and M. Pavon Valderrama, *Phys. Rev. D* **102**, 011504 (2020), arXiv:1907.11220 [hep-ph].
- [42] Y.-W. Pan, M.-Z. Liu, and L.-S. Geng, *Phys. Rev. D* **102**, 054025 (2020), arXiv:2004.07467 [hep-ph].
- [43] P. Junnarkar and N. Mathur, *Phys. Rev. Lett.* **123**, 162003 (2019), arXiv:1906.06054 [hep-lat].
- [44] R. Aaij et al. (LHCb), (2020), arXiv:2012.10380 [hep-ex].
- [45] M.-Z. Liu, Y.-W. Pan, and L.-S. Geng, *Phys. Rev. D* **103**, 034003 (2021), arXiv:2011.07935 [hep-ph].
- [46] Y.-H. Lin and B.-S. Zou, *Phys. Rev. D* **100**, 056005 (2019), arXiv:1908.05309 [hep-ph].
- [47] J.-X. Lu, M.-Z. Liu, R.-X. Shi, and L.-S. Geng, (2021), arXiv:2104.10303 [hep-ph].
- [48] A. Faessler, T. Gutsche, V. E. Lyubovitskij, and Y.-L. Ma, *Phys. Rev. D* **76**, 014005 (2007), arXiv:0705.0254 [hep-ph].
- [49] A. Faessler, T. Gutsche, V. E. Lyubovitskij, and Y.-L. Ma, *Phys. Rev. D* **76**, 114008 (2007), arXiv:0709.3946 [hep-ph].
- [50] A. Faessler, T. Gutsche, V. E. Lyubovitskij, and Y.-L. Ma, *Phys. Rev. D* **77**, 114013 (2008), arXiv:0801.2232 [hep-ph].
- [51] c.-J. Xiao, D.-Y. Chen, and Y.-L. Ma, *Phys. Rev. D* **93**, 094011 (2016), arXiv:1601.06399 [hep-ph].
- [52] Y.-b. Dong, A. Faessler, T. Gutsche, and V. E. Lyubovitskij, *Phys. Rev. D* **77**, 094013 (2008), arXiv:0802.3610 [hep-ph].
- [53] Y. Dong, A. Faessler, T. Gutsche, S. Kovalenko, and V. E. Lyubovitskij, *Phys. Rev. D* **79**, 094013 (2009), arXiv:0903.5416 [hep-ph].
- [54] Q.-F. Lü and Y.-B. Dong, *Phys. Rev. D* **93**, 074020 (2016), arXiv:1603.00559 [hep-ph].
- [55] Y.-H. Lin, C.-W. Shen, and B.-S. Zou, *Nucl. Phys. A* **980**, 21 (2018), arXiv:1805.06843 [hep-ph].
- [56] C.-J. Xiao, D.-Y. Chen, Y.-B. Dong, and G.-W. Meng, *Phys. Rev. D* **103**, 034004 (2021), arXiv:2009.14538 [hep-ph].

- [57] T. Gutsche and V. E. Lyubovitskij, Phys. Rev. D **100**, 094031 (2019), arXiv:1910.03984 [hep-ph].
- [58] S. Weinberg, Phys. Rev. **130**, 776 (1963).
- [59] A. Salam, Nuovo Cim. **25**, 224 (1962).
- [60] K. Hayashi, M. Hirayama, T. Muta, N. Seto, and T. Shirafuji, Fortsch. Phys. **15**, 625 (1967).
- [61] M. Tanabashi et al. (Particle Data Group), Phys. Rev. **D98**, 030001 (2018).
- [62] M.-Z. Liu, T.-W. Wu, J.-J. Xie, M. Pavon Valderrama, and L.-S. Geng, Phys. Rev. **D98**, 014014 (2018), arXiv:1805.08384 [hep-ph].
- [63] Y. Yamaguchi, S. Ohkoda, S. Yasui, and A. Hosaka, Phys. Rev. **D84**, 014032 (2011), arXiv:1105.0734 [hep-ph].
- [64] C.-J. Xiao, D.-Y. Chen, Y.-B. Dong, W. Zuo, and T. Matsuki, Phys. Rev. **D99**, 074003 (2019), arXiv:1811.04688 [hep-ph].